Weak Localization and Light Scattering from Disordered Solids

M. Kaveh, M. Rosenbluh, I. Edrei, and I. Freund
Department of Physics, Bar-Ilan University, Ramat-Gan, Israel
(Received 12 June 1986)

We report the first observation of weak localizations effects in light scattering by a disordered solid. For a diffuse solid scatterer we predict and observe (i) multiple backscattering speckle, (ii) a coherent backscattered peak remaining after removal of this speckle by ensemble averaging, and (iii) speckle statistics which differ from those for single scattering. Computer simulations based upon the theoretical equations yield results in good agreement with experiment.

PACS numbers: 71.55.Jv, 42.20.−y

Lately there has been considerable interest[1-3] in the relationship between Anderson localization[4,5] and light scattering. In particular, it was recently demonstrated[6,7] experimentally that the backscattering intensity of light from polystyrene spheres suspended in water is enhanced by about a factor of 2, resulting in a very narrow peak. This was interpreted[6-8] as due to the phenomenon of weak localization first introduced[5,9] in the transport theory of disordered systems. This phenomenon led[10] to a breakdown of Boltzmann-transport theory for disordered systems and to new universal length-scale–dependent conductivity in two and three dimensions.[5,11,12] Weak localization[13] was also applied recently[14,15] to small microstructures and led[16,17] to new quantum interference phenomena which result in universal oscillations of the magneto-conductance as a function of magnetic field with periods h/e and $h/2e$.

In this Letter we apply the phenomenon of weak localization to light scattering from a disordered solid and show that the intensity is a rapidly fluctuating function of angle with a characteristic period of the order of the wavelength of light, λ, divided by the size of the sample. An ensemble average of the intensity removes these oscillations, leaving a coherent backscattering peak similar to that observed recently[6,7] for disordered fluids. We succeeded in performing this ensemble average experimentally and were thus able to verify this prediction. We also discuss the unique intensity statistics of the oscillations, perform a computer simulation, and again find general agreement with experiment.

The weak localization effect implies that in multiple scattering of light from point $\mathbf{r}_l$ in the disordered solid to point $\mathbf{r}_m$, one must also have a *time-reversal* loop from $\mathbf{r}_m$ to $\mathbf{r}_l$. If the incident-light wave vector is $\mathbf{k}_i$ and the reflected wave vector is $\mathbf{k}_f$, the electric field resulting from these time-reversal loops is given by

$$E_{lm} = E_l P_{lm} \exp[i(\mathbf{k}_i \cdot \mathbf{r}_l - \mathbf{k}_f \cdot \mathbf{r}_m)] + E_m P_{ml} \exp[i(\mathbf{k}_i \cdot \mathbf{r}_m - \mathbf{k}_f \cdot \mathbf{r}_l)], \tag{1}$$

where P_{lm} is the amplitude probability $|P_{lm}|\exp(i\phi_{lm})$ that a given loop between $\mathbf{r}_l$ and $\mathbf{r}_m$ has acquired a phase ϕ_{lm}. From time reversal, $P_{lm} = P_{ml}$. If we assume elastic scattering and no absorption so that $E_l \sim E_m$, the scattered intensity may be written

$$I = I_0\left\{1 + \left[\sum_{l,m} |P_{lm}|^2\right]^{-1}\left[\sum_{l>m} |P_{lm}|^2 \cos[(\mathbf{k}_f + \mathbf{k}_i)\cdot(\mathbf{r}_l - \mathbf{r}_m)] + C(\mathbf{k}_f)\right]\right\}, \tag{2}$$

where

$$C(\mathbf{k}_f) = 2\sum_{l}\sum_{m<l'}\sum_{l'}\sum_{m'<l'} |P_{lm}||p_{l'm'}|\cos[\mathbf{k}_i\cdot(\mathbf{r}_l - \mathbf{r}_{l'}) + \mathbf{k}_f\cdot(\mathbf{r}_{m'} - \mathbf{r}_m) + \phi_{lm} - \phi_{l'm'}]. \tag{3}$$

The second (diagonal) term in Eq. (2) leads to a narrow backscattering peak of width $\Delta\theta_1 \sim \lambda/l_0$, where l_0 is the mean loop length. The third (off diagonal) term $C(\mathbf{k}_f)$ produces large random oscillations with a characteristic width $\Delta\theta_2 \sim \lambda/L_0$, where L_0 is the size of the sample. Obviously, $\langle C(\mathbf{k}_f)\rangle = 0$, where the angular brackets stand for an ensemble average over scatterer positions, so that for a fluid these oscillations are damped out and one observes only the first two terms in Eq. (2), which lead to the coherent backscattering peak. However, for a solid it is not justified to take an ensemble average, and for any particular sample we expect these oscillations to show up, resulting in a backscattering speckle pattern. Accordingly, in our theory we extend previous treatments[8] which were restricted to fluids in which the neglect of the off-diagonal terms is fully justified on the time scale of current experiments.[6,7]

The amplitude probabilities P_{lm} are time dependent, describing the exit from the sample at time t of photons which started their random walk at some earlier time t'. For a random walk with an absorbing plane at $z = 0$, we have

$$|P_{lm}(t,t')|^2 = 4\pi z_l z_m [4\pi(t-t')D]^{-5/2} \exp\{-|\mathbf{r}_l - \mathbf{r}_m|^2/4(t-t')D\}, \tag{4}$$

where the diffusion coefficient D is related to the optical mean free path l by $D=\frac{1}{3}cl$. The intensity at any scattering angle θ represents a time average over some measuring interval Δt, so that the experimental data correspond to

$$I(\theta)=\frac{1}{\Delta t}\int_{\Delta t}dt\int_{-\infty}^{t}I(\theta,t,t')\,dt', \tag{5}$$

where $I(\theta,t,t')$ is the intensity I of Eq. (2) with the time and angle dependence written out explicitly. The diagonal term in Eq. (2) does not depend upon the phases ϕ_{lm}, and the time integrations simply introduce a weighting factor $|P_{lm}|^2\propto|\mathbf{r}_l-\mathbf{r}_m|^{-3}$. When the optical mean free path is very large compared to λ, then $I(\theta,t,t')$ is essentially stationary in time resulting in large amplitude fluctuations as a function of θ, so that in this limit a well-developed speckle pattern is predicted. As the mean free path approaches λ, the θ dependence of $I(\theta,t,t')$ fluctuates rapidly with time and the time integrations of Eq. (5) damp out the speckle pattern. These predictions were verified by numerical simulations and are in accord with the experimental data presented below.

Coherent backscattering was measured by use of a number of different laser lines: Here we present data for the 515-nm line of an argon-ion laser. Kodak White Reflectance Standard,[18] a nonabsorbing, nearly perfectly diffuse scatterer composed of $BaSO_4$ microparticles, was used as the sample. Scanning electron microscopy revealed the microparticles to be generally smooth surfaced, densely packed, and apparently partially oriented, with typically 1-μm diameters and variable lengths. Only minimal traces of interparticle binder were found. We observed that the nature of the results varied with the quality of the scattering surface: The data presented here are for what we judge to be our best sample. The detector-sample distance was ~ 15 m, and the backscattered radiation was scanned along a line which was perpendicular to and passed just above the laser beam. Accordingly, our data do not quite reach zero backscattering angle, but miss this by ~ 300 μrad. A long-focal-length lens translated the 1-W TEM_{00} laser-beam waist downstream to the sample, leading to an ~ 200-μrad far-field diffraction angle. The angular resolution of the detection system itself was ~ 50 μrad.

The experimental results are displayed in Fig. 1. The data shown in Fig. 1(a) were obtained when the sample was rapidly rotated about its surface normal, equivalent to performing an ensemble average in Eq. (3). When the analyzing polarizer was oriented parallel to the laser polarization a broad (20-mrad half-width), well-defined, coherent backscattered peak was observed, while virtually no coherent backscattering was seen for the perpendicular configuration. The lower half of the line shape of the coherent peak

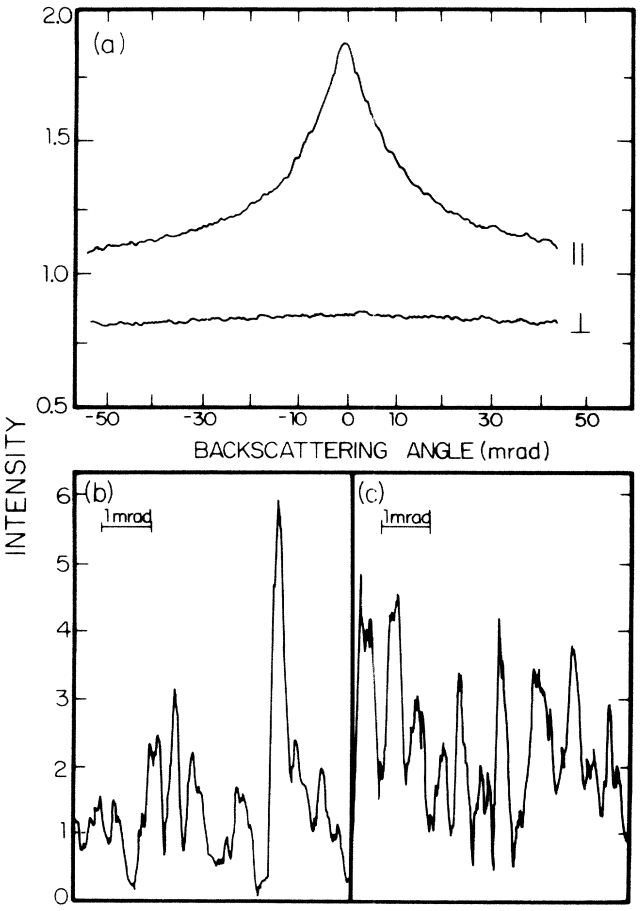

FIG. 1. (a) Coherent backscattered peak for rotating sample with analyzing polarizer oriented either parallel (||) or perpendicular (⊥) to the incident laser polarization. (b),(c) Typical speckle patterns for stationary sample for (b) the wings, and (c) the maximum of the peak of (a). The intensity scale is the same for all three parts.

matches extremely well the very recent predictions of Akkermans, Wolf, and Maynard.[8] Their Eq. (4), when fitted to the data, yields an average loop length for our sample of 4.7 μm. There exists, however, a real discrepancy in the region of the peak maximum which cannot be attributed to instrumental effects. Because of experimental limitations and the extremely slow falloff of intensity in the wings of the backscattered peak, we could not directly measure the ordinary multiple scattering at very large angles which sets the level of unity on the intensity scale. We found, however, that in full accord with theory[8] the wings fall off inversely with momentum transfer, so that a plot of intensity versus $1/\theta$ yielded an extremely good straight line, which, via a least-squares extrapolation, permitted an accurate determination of the background level.

With the sample stationary we observed parallel polarized, free-space backscattering speckle patterns, typical examples of which are shown in Fig. 1(b) for the

wings ($\theta \simeq 50$ mrad), and in Fig. 1(c) for the maximum ($\theta \simeq 0$), of the coherent backscattered peak. Since in our apparatus the detector area is about one-tenth the characteristic area of a speckle cell, the data obtained are essentially undistorted. We verified directly that the measured speckle patterns were reproducible and were not smeared out by either laser-beam instabilities or instrumental vibration.

The statistical properties of the scattering process are reflected in the statistics of the off-diagonal terms in Eq. (3), and thus in the intensity statistics of the backscattered speckle. The fundamental first-order measure of intensity statistics is the probability density $\pi(I)$ of obtaining an intensity between I and $I+dI$. A closely related, widely used, and experimentally more accessible measure is the probability $P(I)$ that the intensity exceeds some threshold value I, i.e., $P(I) = \int_I^\infty \pi(I')\,dI'$; this is the experimental quantity we determine here.

We have examined whether $P(I)$ is measurably different at the peak of the backscattered curve and in the wings by analyzing data for fifteen pairs of scans of speckle intensity versus scattering angle, such as those shown in Figs. 1(b) and 1(c). Each scan pair was for a different sample area and included a narrow angular window in the wings, 45–52 mrad, and a narrow window covering the central upper part of the backscattered peak, -3.5 to $+3.5$ mrad. The experimental results, involving some 3000 measurements of intensity, are plotted for these two regions in Fig. 2 as a function of $I/\langle I\rangle$, where $\langle I\rangle$ is the average intensity of the corresponding region: This permits a direct comparison of $P(I)$ for the two regions. Within the present level of experimental error $P(I)$ appears to be the same for both the peak and the wings.

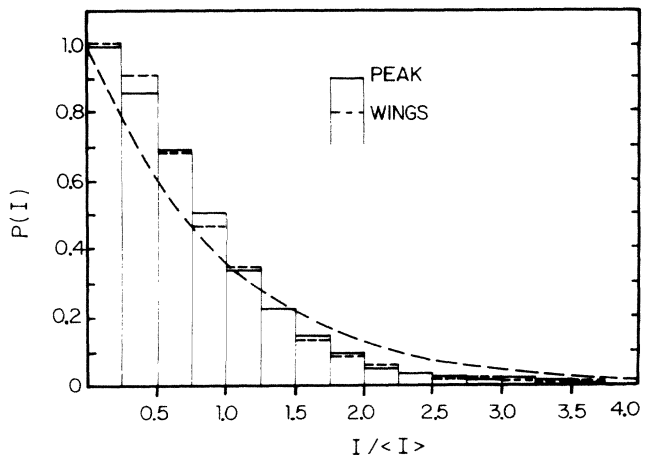

If the optical mean free path and average loop size are many times greater than the wavelength of the light, the background speckle intensity should obey negative exponential statistics, i.e., $\pi(I) = (1/\langle I\rangle) \times \exp(-I/\langle I\rangle)$, $P(I) = \exp(-I/\langle I\rangle)$. Such statistics were first introduced into single scattering speckle theory by Goodman.[19] However, as is evident from Fig. 2, the experimental $P(I)$ differs markedly from a negative exponential, implying a similar marked deviation also for the underlying $\pi(I)$. This difference could easily be observed visually. Perfect negative exponential speckle consists of well-separated bright and dark areas having a wide variation in intensity. The speckle cells observed here, however, appeared as diffuse islands of light which tended both to merge one into another and to be of similar intensity. Since the degree of connectivity of the speckle pattern we obtained here differs so noticeably from that of negative exponential speckle, we suggest that the connectivity of speckle patterns will prove to be a useful parameter in their characterization.

We analyze our data in terms of the gamma density distribution introduced into optical statistics many years ago by Mandel.[20] This takes the form

$$\pi(I) = \left[\frac{\mu}{\langle I\rangle}\right]^{\mu} \frac{I^{\mu-1}\exp[-\mu I/\langle I\rangle]}{\Gamma(\mu)}, \tag{6}$$

and reverts to a negative exponential for $\mu = 1$. Accordingly, deviations of μ from unity can serve as a convenient quantitative first-order measure of the statistical properties of multiple scattered light. Since to the current level of experimental accuracy $P(I)$ is the same in both the peak and the wings of the backscattering, we averaged the measured data for these two areas to obtain a representative distribution for the backscattered region, calculated $P(I)$ by using Eq. (6) for $\pi(I)$ while varying μ, and performed a fit to the data. The results are shown in Fig. 3(a) for $\mu = 2.5$. The corresponding calculated $\pi(I)$ is shown in Fig. 3(b) and emphasizes just how drastic is the departure from negative exponential statistics.

Numerical simulation of Eqs. (2) and (3) for an optical mean free path $l \gg \lambda$ yielded calculated speckle patterns with the expected negative exponential statistics. When we assumed a mean free path $l \sim 2\lambda$, consistent with the large width of the coherent backscattered peak of Fig. 1(a) and the microstructure of our dense solid scatter, the calculated speckle patterns had nonexponential statistics which closely mimicked the experimental results of Fig. 3. Nonexponential statistics are thus observed to be a unique result of the strong multiple scattering, corresponding to a short optical mean free path.

We conclude by considering the question of what characterizes a perfect, diffuse scatterer, i.e., one which scatters light uniformly in all directions. Our

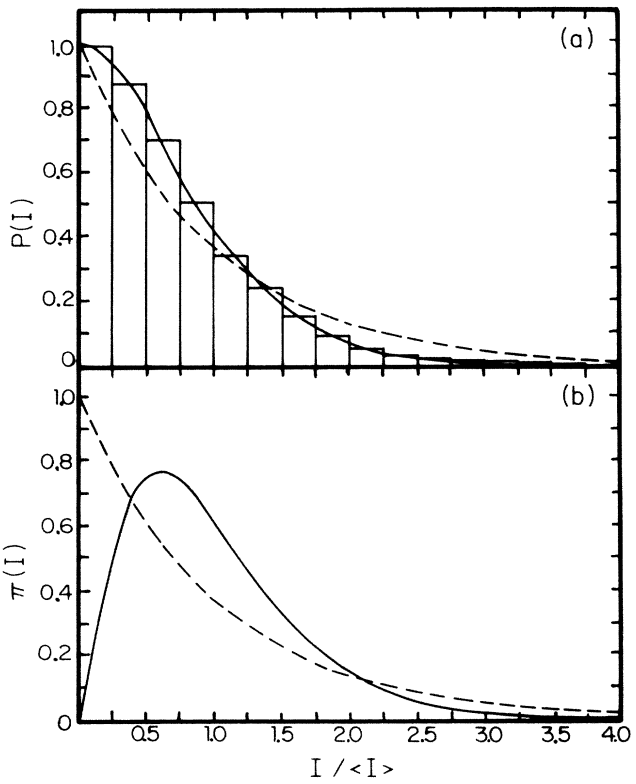

FIG. 3. (a) Intensity statistics $P(I)$ of the backscattered speckle averaged over the peak and wings of the coherent backscattering. The solid curve is a fit of the gamma density distribution, Eq. (6), with $\mu = 2.5$. The dashed curve corresponds to negative exponential statistics. (b) Probability density $\pi(I)$. The dashed curve corresponds to negative exponential statistics, the solid curve to the gamma density distribution for $\mu = 2.5$.

experimental results suggest that for such a scatterer both μ, Eq. (6), and the width of the coherent backscattered peak, Fig. 1(a), diverge. Theory suggests that this occurs at the Anderson transition[1] when the optical mean free path approaches the wavelength of light. It may prove possible to realize this regime experimentally.

[1]S. John, Phys. Rev. Lett. **53**, 2169 (1984); P. W. Anderson, Philos. Mag. B **52**, 505 (1985).

[2]A. A. Golubentzev, Zh. Eksp. Teor. Fiz. **86**, 47 (1984) [Sov. Phys. JETP **59**, 26 (1984)]; E. Akkermans and R. Maynard, J. Phys. (Paris), Lett. **46**, L1045 (1985).

[3]M. J. Stephen, Phys. Rev. Lett. **56**, 1809 (1986).

[4]P. W. Anderson, Phys. Rev. **109**, 1492 (1958).

[5]E. Abrahams, P. W. Anderson, D. C. Licciardello, and T. V. Ramakrishnan, Phys. Rev. Lett. **42**, 673 (1979).

[6]M. P. Van Albada and A. Lagendijk, Phys. Rev. Lett. **55**, 2692 (1985).

[7]P. E. Wolf and G. Maret, Phys. Rev. Lett. **55**, 2696 (1985).

[8]E. Akkermans, P. E. Wolf, and R. Maynard, Phys. Rev. Lett. **56**, 1471 (1986).

[9]L. P. Gor'kov, A. F. Larkin, and D. E. Khmel'nitskiĭ, Pis'ma Zh. Eksp. Teor. Fiz. **30**, 248 (1979) [JETP Lett. **30**, 228 (1979)].

[10]For reviews, see P. A. Lee and T. V. Ramakrishnan, Rev. Mod. Phys. **57**, 287 (1985); N. F. Mott and M. Kaveh, Adv. Phys. **34**, 329 (1985).

[11]G. D. Bergmann, Phys. Rev. B **28**, 2914 (1983); M. Kaveh, M. Uren, R. A. Davies, and M. Pepper, J. Phys. C **14**, L413 (1981); for a review, see G. Bergmann, Phys. Rep. **107**, 1 (1984).

[12]A. Kawabata, Solid State Commun. **38**, 823 (1981); M. Kaveh and N. F. Mott, J. Phys. C **15**, L707 (1982). For a recent review, see G. A. Thomas, Philos. Mag. **52**, 479 (1985).

[13]For a review of theoretical and experimental observations, see Bergmann, Ref. 11.

[14]B. L. Al'tshuler, A. G. Aronov, and B. Z. Spivak, Pis'ma Zh. Eksp. Teor. Fiz. **33**, 101 (1981) [JETP Lett. **33**, 94 (1981)]; for a review, see Yu. Sharvin, Physica (Amsterdam) **126B+C**, 228 (1984).

[15]M. Büttiker, Y. Imry, and R. Landauer, Phys. Lett. **96A**, 365 (1983); Y. Gefen, Y. Imry, and M. Ya. Azbel, Phys. Rev. Lett. **52**, 129 (1984); M. Büttiker, Y. Imry, R. Landauer, and S. Pinhas, Phys. Rev. B **31**, 6207 (1985).

[16]B. L. Al'tshuler, A. G. Aronov, B. Z. Spivak, D. Yu. Sharvin, and Yu. V. Sharvin, Pis'ma Zh. Teor. Fiz. **35**, 476 (1982) [JETP Lett. **35**, 588 (1982)]. For universal conductance fluctuations, see A. D. Stone, Phys. Rev. Lett. **54**, 2692 (1985); P. A. Lee and A. D. Stone, Phys. Rev. Lett. **55**, 1622 (1985); S. Feng, P. A. Lee, and A. D. Stone, Phys. Rev. Lett. **56**, 1960 (1986).

[17]R. A. Webb, S. Washburn, C. P. Umbach, and R. B. Laibowitz, Phys. Rev. Lett. **54**, 2696 (1985); V. Chandrasekhar, M. J. Rooks, S. Wind, and D. E. Prober, Phys. Rev. Lett. **55**, 1610 (1985). For a recent observation of universal conductance fluctuations, see W. J. Skocpol, P. M. Mankiewich, R. E. Howard, L. D. Jackel, D. M. Tennat, and A. D. Stone, Phys. Rev. Lett. **56**, 2865 (1986).

[18]Eastman Kodak Company, Rochester, NY 14650.

[19]J. W. Goodman, Proc. IEEE **55**, 1688 (1965).

[20]L. Mandel, Proc. Phys. Soc. **74**, 233 (1959).